Organic anion transporting polypeptide 1a/1b–knockout mice provide insights into hepatic handling of bilirubin, bile acids, and drugs

Evita van de Steeg,[1] Els Wagenaar,[1] Cornelia M.M. van der Kruijssen,[1] Johanna E.C. Burggraaff,[1] Dirk R. de Waart,[2] Ronald P.J. Oude Elferink,[2] Kathryn E. Kenworthy,[3] and Alfred H. Schinkel[1]

[1]Division of Molecular Biology, The Netherlands Cancer Institute, Amsterdam, The Netherlands. [2]Tytgat Institute for Liver and Intestinal Research, Academic Medical Center, Amsterdam, The Netherlands. [3]Department of Drug Metabolism and Pharmacokinetics, GlaxoSmithKline, Ware, United Kingdom.

Organic anion transporting polypeptides (OATPs) are uptake transporters for a broad range of endogenous compounds and xenobiotics. To investigate the physiologic and pharmacologic roles of OATPs of the 1A and 1B subfamilies, we generated mice lacking all established and predicted mouse Oatp1a/1b transporters (referred to as *Slco1a/1b−/−* mice, as *SLCO* genes encode OATPs). *Slco1a/1b−/−* mice were viable and fertile but exhibited markedly increased plasma levels of bilirubin conjugated to glucuronide and increased plasma levels of unconjugated bile acids. The unexpected conjugated hyperbilirubinemia indicates that Oatp1a/1b transporters normally mediate extensive hepatic reuptake of glucuronidated bilirubin. We therefore hypothesized that substantial sinusoidal secretion and subsequent Oatp1a/1b-mediated reuptake of glucuronidated compounds can occur in hepatocytes under physiologic conditions. This alters our perspective on normal liver functioning. *Slco1a/1b−/−* mice also showed drastically decreased hepatic uptake and consequently increased systemic exposure following i.v. or oral administration of the OATP substrate drugs methotrexate and fexofenadine. Importantly, intestinal absorption of oral methotrexate or fexofenadine was not affected in *Slco1a/1b−/−* mice. Further analysis showed that rifampicin was an effective and specific Oatp1a/1b inhibitor in controlling methotrexate pharmacokinetics. These data indicate that Oatp1a/1b transporters play an essential role in hepatic reuptake of conjugated bilirubin and uptake of unconjugated bile acids and drugs. *Slco1a/1b−/−* mice will provide excellent tools to study further the role of Oatp1a/1b transporters in physiology and drug disposition.

Introduction

Organic anion transporting polypeptides (human: OATP, gene *SLCO*; rodents: Oatp, gene *Slco*) belong to the superfamily of the solute carrier class of organic anion transporters (1). This OATP/Oatp superfamily consists of 6 different families, which can be further subdivided into subfamilies based on their amino acid sequence identity (1). Currently, 11 human OATPs and 15 mouse Oatps have been identified (2). OATPs/Oatps facilitate sodium-independent uptake transport of a wide variety of organic endo- and exogenous compounds, such as bile acids, steroid and thyroid hormones and their conjugates, and numerous drugs and toxins (for overview, see refs. 3, 4). Because of this broad substrate specificity and due to their expression in pharmacokinetically important tissues (liver, small intestine, kidney), OATPs/Oatps of the 1A/1a and 1B/1b subfamilies are thought to play an important role in drug disposition.

There is currently a profound interest in further understanding the contribution of OATP transporters to drug disposition in vivo. Members of the OATP1A/1B family are highly expressed in the sinusoidal membrane of hepatocytes or in the apical membrane of enterocytes where they might affect liver penetration or intestinal uptake, respectively, of drugs, xenobiotics, and

endogenous substances (1, 5). Pharmacological inhibition of these transporters could therefore be used to lower the hepatic concentrations of certain drugs (for instance, to prevent hepatotoxicity) or to increase their systemic exposure. This might be advantageous for some drugs, but for other drugs, this might give rise to unforeseen toxic side effects. OATP1A/1Bs therefore also present a significant factor in drug-drug interactions. Additionally, various SNPs have been identified in human *SLCO1A/1B* genes, especially in *SLCO1B1*, some of which have been associated with increased plasma levels of statins and irinotecan in patients, sometimes resulting in severe and life-threatening toxicity (6–8). Genetic variation in *SLCO1A/1B* genes, resulting in altered transport activity, might therefore be an important factor in interindividual variation in response to drug treatment.

Only recently, mouse models have been generated to study OATPs/Oatps in vivo. For example, single *Slco1b2−/−* mice have been generated and used to study the role of Oatp1b2 in plasma and liver distribution of toxins (phalloidin, microcystin-LR), statins (cerivastatin, lovastatin acid, pravastatin, and simvastatin acid) and antibiotics (rifampicin and rifamycin SV) (2, 9, 10). Furthermore, our group recently generated and characterized OATP1B1 transgenic mice, in which OATP1B1-mediated hepatic uptake of methotrexate (MTX) was demonstrated in vivo (11).

The aim of this study was to increase our knowledge of the physiological and pharmacological roles of the Oatp1a/1b trans-
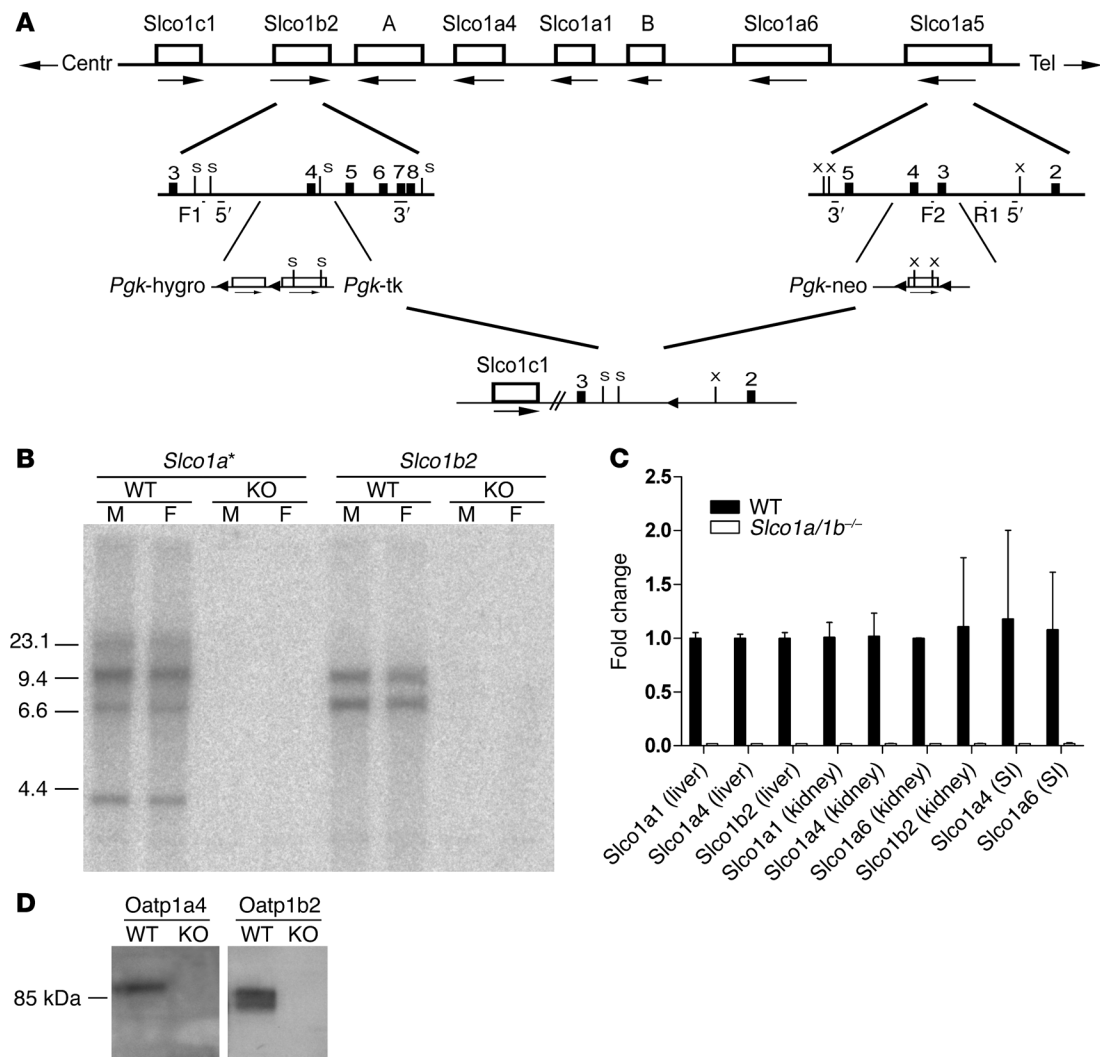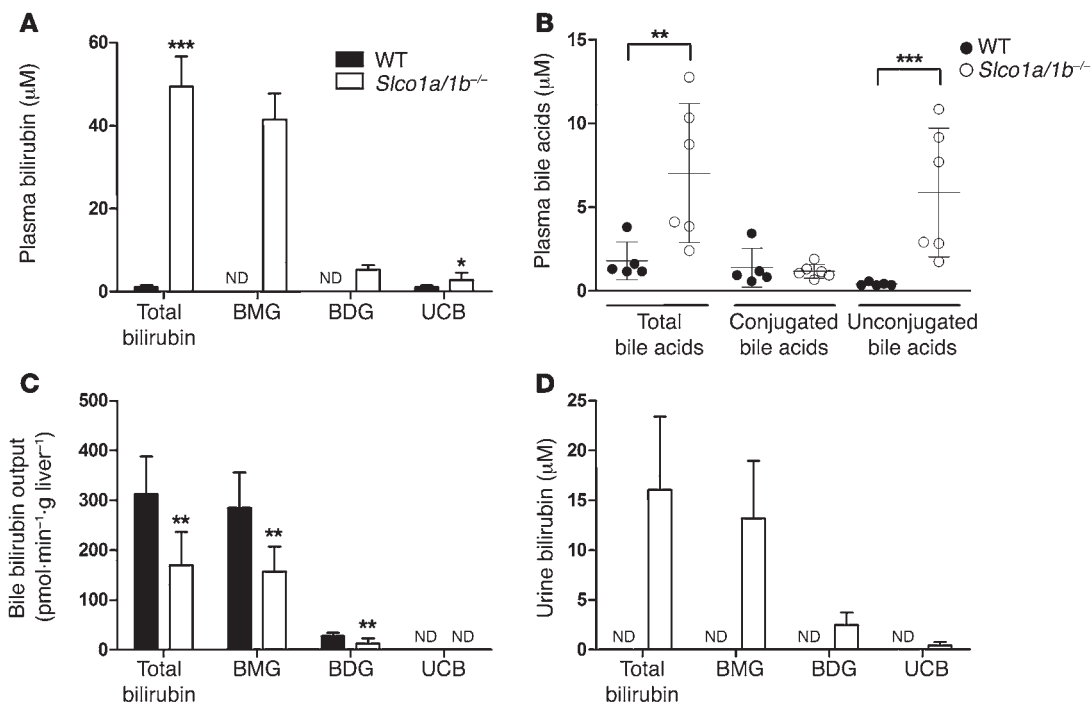
Figure 1
Generation of *Slco1a/1b*[−/−] mice. (**A**) To delete all the *Slco1a* and *Slco1b* genes, an inverted *Pgk*-neomycin cassette with *loxP* sequences was inserted, replacing exons 3 and 4 of *Slco1a5*. Additionally, a *Pgk*-thymidine kinase and a *Pgk*-hygromycin cassette with *loxP* sequences were inserted, replacing exon 4 of *Slco1b2*. The *Slco1a/1b* cluster was subsequently excised from the genome by *Pgk-Cre* recombinase transfection. Structure of the region after deletion of the *Slco1a/1b* cluster is shown as well. Probes (5′ and 3′) used for Southern blot analyses (positioned outside the respective targeting constructs) and forward (F1 and F2) and reverse (R1) primers used for PCR analyses are indicated by lines below the DNA backbone. Gene *A* and gene *B* represent *Slco1a*-like predicted genes EG435927 and EG625716 (according to the NCBI database), respectively. Triangles indicate *loxP* sequences, numbered boxes indicate exons, and arrows indicate transcriptional orientation. Centr, centromere; Tel, telomere; S, SacI; X, XbaI. (**B**) Southern blot analysis of tail DNA from WT and *Slco1a/1b*[−/−] mice digested with Asp718 and probed with partial *Slco1a** or *Slco1b2* cDNA. (**C**) RT-PCR analysis of *Slco1a/1b* genes in liver, kidney, and small intestine (SI) of WT and *Slco1a/1b*[−/−] mice. (**D**) Western blot analysis of crude membrane fractions of livers derived from WT and *Slco1a/1b*[−/−] mice. Blots were probed with either an antibody raised against mouse Oatp1a4 (sc-18436) or Oatp1b2 (sc-47270).

porters in vivo. Since the various Oatp1a and Oatp1b transporters display a large overlap in tissue distribution and substrate specificity (1), we considered that making single gene knockouts would easily result in redundancy or compensation. Moreover, within the OATP1A/1B family, there are no straightforward orthologous genes between humans and rodents. For instance, OATP1A2 is the only human member of the OATP1A subfamily, whereas rats and mice have several members (Oatp1a1, -1a4, 1a5, and -1a6), most likely due to gene duplication events (5). Conversely, OATP1B1 and OATP1B3 are the 2 human members of the OATP1B subfamily, with Oatp1b2 being the only rodent ortholog (5). For these

reasons, we generated and subsequently characterized a mouse model that is functionally deficient for all 5 established *Slco1a* and *Slco1b* genes (*Slco1a/1b*[−/−] mice).

Results

Generation and characterization of Slco1a/1b cluster knockout mice. *Slco1a/1b*[−/−] mice were generated using insertion of *loxP* sites at both ends of the *Slco1a/1b* gene cluster (~620 kb), followed by *Cre*-mediated deletion (Figure 1A and Supplemental Methods; supplemental material available online with this article; doi:10.1172/JCI42168DS1). We chose not to delete the adjacent *Slco1c1* gene, as

Figure 2
Analysis of plasma, bile, and urine from male WT and *Slco1a/1b*−/− mice. Levels of total bilirubin, BMG, BDG, and UCB in plasma (**A**), bile (**C**), and urine (**D**) and levels of total bile acids, conjugated bile acids, and unconjugated bile acids in plasma (**B**) are shown. Bile was collected for 15 minutes after gallbladder cannulation and ligation of the common bile duct. Urine was collected by spot sampling from nonanesthetized mice. Data are presented as mean ± SD (n = 5–7; *$P < 0.05$; **$P < 0.01$; ***$P < 0.001$ when compared with WT). ND, not detectable; detection limits were 0.3 μM for plasma and urine and 2 μM for bile, i.e., ~5 pmol•min−1•g liver−1.

its selective substrate specificity, its relative conservation between mouse and human, and its primary expression in brain and testis (1) point to a specific physiological function in these organs, possibly thyroid hormone uptake.

The *Slco1a/1b* gene cluster consists of 5 established *Slco1a* and -*1b* genes and 2 *Slco1a*-like predicted genes (EG435927 and EG625716 according to the NCBI database; *A* and *B* in Figure 1A). Complete deletion of all genes within the cluster was confirmed by Southern blot analysis (Figure 1B) of WT and *Slco1a/1b*−/− genomic DNA using a generic *Slco1a* cDNA (cross-hybridizing with *Slco1a1*, -*1a4*, -*1a5*, and -*1a6*) or *Slco1b2* cDNA probe. The extensive hybridization present in WT mice was absent in *Slco1a/1b*−/− mice. Additional RT-PCR analysis demonstrated a sharp "downregulation" of *Slco1a1*, -*1a4*, and -*1b2* in livers and *Slco1a1* and -*1a6* in kidneys of *Slco1a/1b*−/− mice compared with WTs (Figure 1C). Whereas in WT mice, we found some expression of *Slco1a4* and *Slco1a6* in the small intestine and of *Slco1a4* and *Slco1b2* in the kidney, this was absent in *Slco1a/1b*−/− mice (Figure 1C and Supplemental Table 1). Western blotting confirmed absence of Oatp1a4 and Oatp1b2 protein in *Slco1a/1b*−/− liver (Figure 1D).

Slco1a/1b−/− mice were viable and fertile and had normal life spans. Both male and female *Slco1a/1b*−/− mice at 9–14 weeks of age, however, had slightly but significantly increased body weights (~1.1-fold; $P < 0.001$; $n > 50$) compared with WT mice. Absolute weights of all major tissues did not differ between the 2 strains (data not shown). Although macro- and microscopic histological and pathological analysis did not reveal obvious aberrations in tissues of *Slco1a/1b*−/− mice at approximately 12 or

85 weeks of age, *Slco1a/1b*−/− mice demonstrated clear jaundice as a consequence of hyperbilirubinemia (see below).

Expression levels of other transporter proteins in tissues of Slco1a/1b−/− *mice.* RT-PCR analysis was performed to determine the expression levels of various uptake and efflux transporters (see Methods) in liver, kidney, and small intestine of male WT and *Slco1a/1b*−/− mice (Supplemental Table 1). Hepatic expression of UDP-glucurono-syltransferase 1a1 (*Ugt1a1*) and aldehyde oxidase 1 and 3 (*Aox1* and *Aox3*) was also determined, since these enzymes catalyze the glucuronidation of bilirubin and oxidation of MTX to 7-hydroxy-methotrexate (7OH-MTX; see below), respectively. We found a modest downregulation (about 2.5-fold) of hepatic *Abcb1a* in *Slco1a/1b*−/− compared with WT mice ($P < 0.05$; Supplemental Table 1). Of all other genes analyzed (other than *Slco1a/1b*), no differences in expression were observed between WT and *Slco1a/1b*−/− mice. Western blot analysis confirmed similar expression levels of Abcc2, Abcc3, Abcc4, and Abcg2 in the livers of WT and *Slco1a/1b*−/− mice (data not shown).

Analysis of blood and plasma of Slco1a/1b−/− *mice.* Hematological examination of male and female *Slco1a/1b*−/− mice (see Methods) revealed no marked abnormalities (data not shown). HPLC analysis of plasma of male *Slco1a/1b*−/− mice, however, demonstrated a more than 40-fold increase in total bilirubin levels compared with WT mice ($P < 0.001$; Figure 2A). Approximately 95% of this increase was due to elevated levels of conjugated bilirubin (~85% bilirubin monoglucuronide [BMG], and ~10% bilirubin diglucuronide [BDG]; both were below the detection limit in WT mice [<0.3 μM]). Unconjugated bilirubin (UCB) levels in plasma were
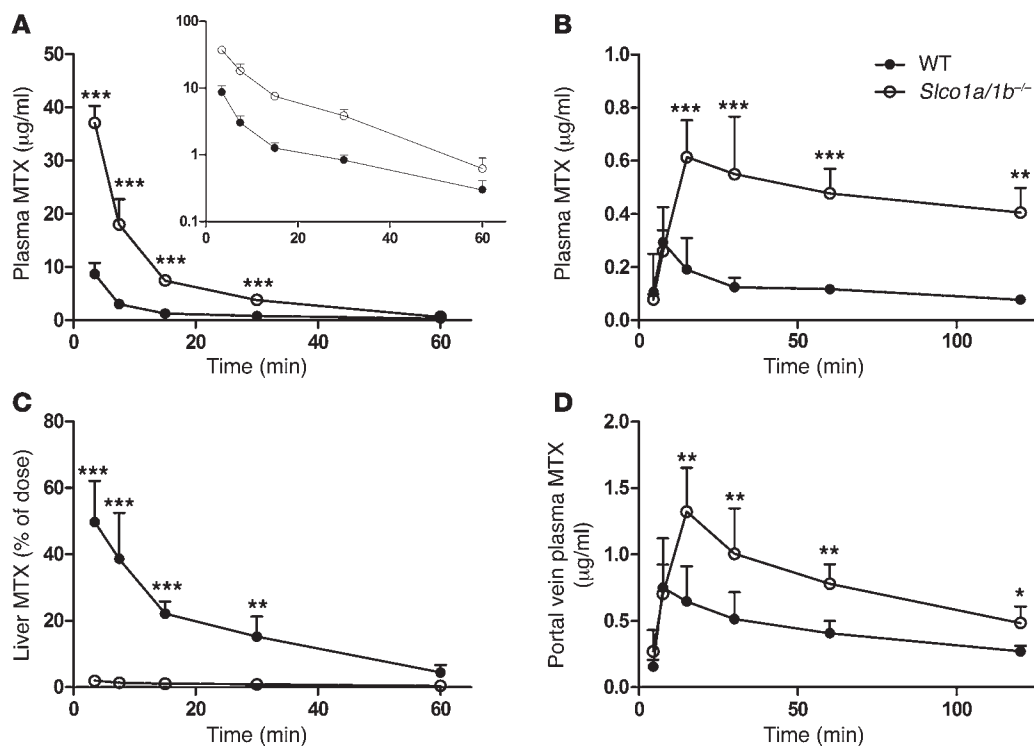
Figure 3
Role of hepatic Oatp1a/1b transporters in MTX disposition. Pharmacokinetics of MTX after i.v. or oral administration of MTX (10 mg/kg) to female WT and *Slco1a/1b⁻/⁻* mice. MTX plasma concentration versus time curves after i.v. (**A**) or oral (**B**) administration, with the inset showing the semi-log plot of the i.v. data. (**C**) MTX liver levels (% of dose) versus time curves after i.v. administration. (**D**) MTX portal vein plasma concentration versus time curves after oral administration. All data are presented as mean ± SD (n = 4–8; *P < 0.05; **P < 0.01; ***P < 0.001 when compared with WT).

also modestly but significantly increased (~2.5-fold) in *Slco1a/1b⁻/⁻* mice compared with WT mice (P < 0.05; Figure 2A). Similar data were found in females (not shown). Interestingly, total bile acid levels in plasma of *Slco1a/1b⁻/⁻* mice were 4-fold increased compared with WT mice (P < 0.05), and this was almost exclusively due to increased levels of unconjugated bile acids (13-fold increase, P < 0.05; Figure 2B and Supplemental Figure 1). Furthermore, moderate but significant increases were observed in plasma HDL cholesterol when comparing *Slco1a/1b⁻/⁻* with WT mice (4.28 ± 0.83 versus 2.97 ± 0.35 [male; P < 0.01] and 3.55 ± 0.38 versus 2.77 ± 0.35 mM [female; P < 0.01]) and in plasma triglyceride levels (1.96 ± 0.53 versus 1.02 ± 0.23 [male; P < 0.001] and 1.87 ± 0.55 versus 1.15 ± 0.30 mM [female; P < 0.05]). No significant differences between knockout and WT plasma were found in any of the other clinical chemical parameters measured (see Methods; data not shown).

Analysis of bile and urine of Slco1a/1b⁻/⁻ mice. Bile composition of male WT and *Slco1a/1b⁻/⁻* mice was measured after ligation of the common bile duct and gall bladder cannulation. Bile flow was unchanged between the 2 strains (~2.3 μl/min/g liver). However, the biliary excretion of total bilirubin was nearly halved (to 54% of WT level) in *Slco1a/1b⁻/⁻* mice compared with WT mice (P < 0.01; Figure 2C). This was caused by reduced biliary excretion of both BMG and BDG. Levels of UCB in bile were below the detection limit in both strains. Analysis of total bile acid and GSH excretion in bile did not show any differences between *Slco1a/1b⁻/⁻* and WT mice (data not shown). The total bile acid pool size in the animals also did not differ between WT and *Slco1a/1b⁻/⁻* mice (35.3 ± 7.1 and 35.7 ± 6.8 μmol, respectively).

Upon collection of urine in a metabolic cage experiment, no differences in standard clinical parameters of urine (see Methods) were found between WT and *Slco1a/1b⁻/⁻* mice, except for total protein, of which the urinary excretion was significantly reduced in *Slco1a/1b⁻/⁻* mice compared with WTs (10.2 ± 2.0 versus 29.9 ± 6.4 mg/24 hours [male; P < 0.01] and 3.0 ± 1.6 versus 10.7 ± 3.0 mg/24 hours [female; P < 0.01]). Due to its instability, bilirubin could not be tested in this experimental setting. Instead, urine was collected by spot sampling from male *Slco1a/1b⁻/⁻* and WT mice. Urinary excretion of bilirubin could only be detected in *Slco1a/1b⁻/⁻* mice, as in WT mice the amount of urinary bilirubin was below the detection limit (<0.3 μM; Figure 2D). The urinary excretion of bilirubin in *Slco1a/1b⁻/⁻* mice reflected the high plasma levels of bilirubin in this strain, with most of the excreted bilirubin in urine being BMG.

Role of Oatp1a/1b proteins in MTX pharmacokinetics. The anticancer and antirheumatic drug MTX is transported in vitro by various members of the OATP1A/1B family (12–14). To determine the role of Oatp1a/1b transporters in MTX disposition in vivo, we administered MTX (10 mg/kg) i.v. or orally to female WT and *Slco1a/1b⁻/⁻* mice. Levels of MTX and 7OH-MTX in plasma and several organs were analyzed by HPLC. Both after i.v. and oral application, systemic plasma AUCs of MTX were markedly (4.8- and 3.8-fold) increased in *Slco1a/1b⁻/⁻* mice compared with WTs (422 ± 17.3 versus 87.3 ± 5.1 min·μg/ml [P < 0.01] and 54.5 ± 2.9 versus 14.4 ± 0.9 min·μg/ml [P < 0.001] after i.v. and oral dosage, respectively; Figure 3, A and B). Interestingly, only 3.5 minutes after i.v. injection of MTX, the effect of Oatp1a/1b transporters was very

Table 1
Levels of MTX in plasma and organs 15 minutes after i.v. administration of MTX to female WT and *Slco1a/1b*[-/-] mice

	WT		*Slco1a/1b*[-/-]		
	Conc.	T/P ratio	Conc.	T/P ratio	WT/KO conc. ratio
Plasma (μg/ml)	1.27 ± 0.2	–	7.47 ± 0.9[A]	–	0.17
Liver (μg/g)	54.5 ± 10	43.1 ± 1.8	2.46 ± 0.5[A]	0.33 ± 0.1[A]	22.1
Kidney (μg/g)	5.23 ± 1.5	3.94 ± 1.3	19.8 ± 6.2[B]	2.64 ± 0.7	0.26
SI (+ contents) (μg/g)	48.7 ± 16	37.1 ± 15	2.93 ± 0.6[A]	0.39 ± 0.1[A]	16.6
Brain (μg/g)	0.08 ± 0.01	0.05 ± 0.02	0.13 ± 0.02[B]	0.02 ± 0.00[C]	0.62
Spleen (μg/g)	0.58 ± 0.03	0.32 ± 0.22	2.29 ± 0.71[B]	0.31 ± 0.10	0.25

MTX administered at 10 mg/kg. All data are presented as mean ± SD (n = 4–7). Conc., concentration; T/P ratio, tissue-to-plasma ratio. [A]$P < 0.001$; [B]$P < 0.01$; [C]$P < 0.05$ when compared with WT.

pronounced, and we found more than 50% of the MTX dose in the WT livers, versus only 2% in *Slco1a/1b*[-/-] livers ($P < 0.001$; Figure 3C). This demonstrates the importance of Oatp1a/1b transporters, especially in early liver uptake and clearance of this drug from the circulation, when plasma levels are high. Whereas plasma levels of MTX 60 minutes after i.v. administration were not significantly different anymore between the 2 strains (Figure 3A), significant differences were maintained for over 2 hours after oral dosing ($P < 0.01$; Figure 3B). The main hepatic and toxic metabolite of MTX, 7OH-MTX, was substantially present in WT plasma (0.03 ± 0.001 μg/ml) and liver (7.85 ± 2.31 μg/g) 15 minutes after i.v. administration of MTX, but undetectable in *Slco1a/1b*[-/-] mice, further underscoring the impact of Oatp1a/1b transporters on MTX pharmaco- and toxicokinetics.

Most likely because of reduced hepatic uptake and consequently reduced biliary excretion in the *Slco1a/1b*[-/-] mice, levels of MTX were also markedly decreased (16.6-fold) in the small intestine and its contents 15 minutes after i.v. administration ($P < 0.001$; Table 1). Levels of MTX in kidney, brain, and spleen in this experiment were higher in *Slco1a/1b*[-/-] mice compared with WTs, reflecting the increased plasma levels (Table 1).

To study the possible role of intestinal Oatp1a/1b transporters (we had detected mRNA of *Slco1a4* and *Slco1a6* in the small intestine) in the oral absorption of MTX, we collected blood samples from the portal vein and the general circulation (cardiac puncture) after oral administration of MTX (10 mg/kg) to WT and *Slco1a/1b*[-/-] mice. No differences in MTX concentrations in the portal vein were found between the 2 strains shortly after dosing (5 and 7.5 minutes) (Figure 3D). At these time points, also the systemic plasma levels (Figure 3B) (and liver levels; Supplemental Figure 2) of MTX did not yet differ between the 2 strains, suggesting low impact of hepatic Oatp1a/1b transporters upon first pass of the drug through the liver. At later time points, however, systemic and portal vein MTX concentrations were significantly higher in the absence of Oatp1a/1b proteins (Figure 3, B and D). Because the differences in portal vein concentrations of MTX between *Slco1a/1b*[-/-] and WT mice appeared to reflect the differences in systemic MTX levels between these strains (Figure 3, B and D, and Supplemental Table 2), it seems likely that the increased levels of MTX in the portal vein of *Slco1a/1b*[-/-] mice at later time points are a secondary consequence of the higher systemic levels of MTX in these mice. We therefore conclude that there is no significant role of Oatp1a/1b proteins in the intestinal absorption of MTX. In accordance with these data,

no significant differences were observed in the amount of drug retrieved from the small intestine and its contents after oral administration (data not shown).

Effect of Oatp1a/1b transporters on urinary and fecal excretion of MTX. In humans and mice, urinary excretion is the prominent route of ultimate MTX elimination, although in mice still approximately 20% of the MTX is excreted unchanged in the feces (15). We collected urine and feces of WT and *Slco1a/1b*[-/-] mice for 24 hours after i.v. administration of MTX (10 mg/kg), using metabolic cages and measured MTX in urine and feces (Figure 4). In *Slco1a/1b*[-/-] mice, virtually the entire MTX dose was excreted via the kidneys (versus ~40% in WT mice; $P < 0.01$) and only approximately 2% of the dose ended up in the feces (versus ~20% in WT mice; $P = 0.07$). These data are in line with the sharply reduced hepatic uptake (and consequently reduced biliary excretion) of MTX in the absence of Oatp1a/1b transporters. These data also show that in the absence of Oatp1a/1b transporters, MTX can still be virtually completely eliminated by the kidneys.

Role of Oatp1a/1b proteins in FEX pharmacokinetics. Fexofenadine (FEX) is an in vitro Oatp1a/1b substrate that is hardly metabolized in humans, and biliary excretion of unchanged FEX is the main elimination route in mice (16). To determine the pharmacokinetic role of Oatp1a/1b transporters after FEX administration in vivo, WT and *Slco1a/1b*[-/-] mice received 1 mg/kg [³H]FEX i.v. or orally, and drug levels were determined by measuring total radioactivity. Results for [³H]FEX were qualitatively comparable to the MTX
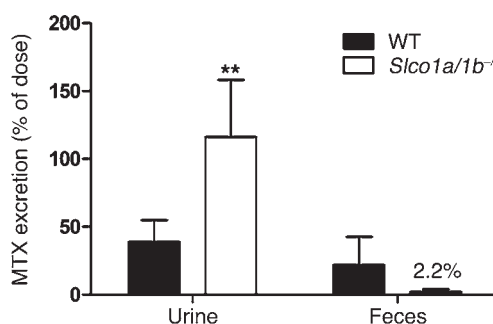
Figure 4
Urinary and fecal excretion of MTX (% of dose) in the first 24 hours after i.v. administration of MTX (10 mg/kg) to male WT and *Slco1a/1b*[-/-] mice. All bars present mean ± SD (n = 6; **$P < 0.01$ when compared with WT).
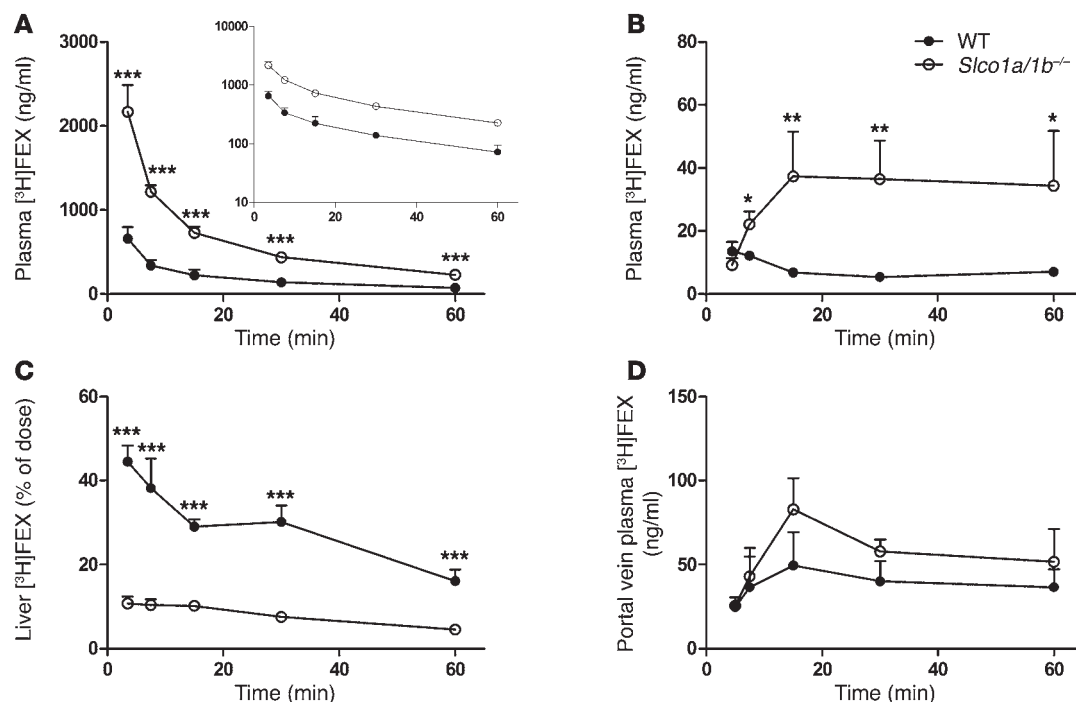
Figure 5
Role of hepatic Oatp1a/1b transporters in FEX disposition. Pharmacokinetics of FEX after i.v. or oral administration of [³H]FEX (1 mg/kg) to male WT and *Slco1a/1b⁻/⁻* mice. (**A**) [³H]FEX plasma concentration versus time curves after i.v. (**A**) or oral (**B**) administration, with the inset showing the semi-log plot of the i.v. data. (**C**) [³H]FEX liver levels (% of dose) versus time curves after i.v. administration. (**D**) [³H]FEX plasma concentration versus time curves after oral administration. All data are presented as mean ± SD ($n = 4–5$; *$P < 0.05$; **$P < 0.01$; ***$P < 0.001$ when compared with WT).

results. Systemic plasma levels of [³H]FEX were 3.3- and 4.6-fold increased in *Slco1a/1b⁻/⁻* mice compared with WTs, with AUCs of 36.5 ± 0.5 versus 11.1 ± 1.0 min·μg/ml ($P < 0.001$) and 1.9 ± 0.2 versus 0.41 ± 0.02 min·μg/ml ($P < 0.01$) after i.v. and oral dosing, respectively (Figure 5, A and B). As with MTX, only 3.5 minutes after i.v. injection of [³H]FEX, a profound effect of Oatp1a/1b transporters on drug uptake into the liver was observed, with more than 45% of the dose present in WT liver versus only 11% in *Slco1a/1b⁻/⁻* liver ($P < 0.001$; Figure 5C). Levels of [³H]FEX in small intestine plus contents of *Slco1a/1b⁻/⁻* mice were 1.6-fold reduced compared with WT mice ($P < 0.01$; Table 2), presumably because of reduced biliary excretion. Levels of [³H]FEX in kidney, brain, and spleen 15 minutes after dosing were higher in *Slco1a/1b⁻/⁻* mice compared with WTs, probably reflecting the increased plasma levels (Table 2).

After oral administration of [³H]FEX, no significant differences were observed in the amounts of drug present in the portal vein between WT and *Slco1a/1b⁻/⁻* mice early after oral administration (5 and 7.5 minutes). At 5 minutes, also the systemic plasma levels (Figure 5B) (and liver levels; Supplemental Figure 2) of FEX did not yet differ between the 2 strains, suggesting low impact of hepatic Oatp1a/1b transporters on first pass of the drug through the liver. At later time points, however, there was a trend toward increased levels of [³H]FEX in the portal vein of *Slco1a/1b⁻/⁻* mice (Figure 5, B and D). As with MTX, this tendency reflected the differences in systemic [³H]FEX levels between WT and *Slco1a/1b⁻/⁻* mice (Supplemental Table 2), implying that the increased levels of [³H]FEX in the portal vein of *Slco1a/1b⁻/⁻* mice are a secondary consequence of increased systemic drug concentrations. There-

fore, as with MTX, we found no indications for a significant role of murine Oatp1a/1b in the intestinal absorption of FEX.

Effect of rifampicin on MTX disposition in WT and Slco1a/1b⁻/⁻ mice. Mice with detoxifying proteins knocked out present ideal tools to assess the specificity and efficacy of pharmacological inhibitors of detoxifying proteins. To determine the efficacy and specificity of the prototypical Oatp1a/1b inhibitor rifampicin, we predosed WT and *Slco1a/1b⁻/⁻* mice with 20 mg/kg rifampicin i.v. 3 minutes before MTX administration (10 mg/kg i.v.). Upon rifampicin treatment, MTX plasma levels in WT mice 15 minutes after MTX administration rose to the same levels as reached in *Slco1a/1b⁻/⁻* mice, whereas no difference was observed between rifampicin-pretreated and nontreated *Slco1a/1b⁻/⁻* mice (Figure 6A). Liver MTX and 7OH-MTX levels were markedly reduced upon rifampicin treatment in WT mice, although not as low as in *Slco1a/1b⁻/⁻* mice, suggesting extensive, but not complete inhibition of Oatp1a/1b transporters by rifampicin in this experiment (Figure 6, B and C). Importantly, there was no effect of rifampicin treatment on plasma or liver MTX levels in *Slco1a/1b⁻/⁻* mice, suggesting specificity of rifampicin for inhibiting Oatp1a/1b proteins in the context of MTX pharmacokinetics.

Discussion
We have generated and characterized what we believe is a novel mouse model lacking all *Slco1a/1b* genes. *Slco1a/1b⁻/⁻* mice were viable, fertile, and did not show clear pathological abnormalities, but displayed marked conjugated hyperbilirubinemia and associated jaundice. The conjugated hyperbilirubinemia was

Table 2

Levels of [³H]FEX equivalents in plasma and organs 15 minutes after i.v. administration of [³H]FEX to male WT and *Slco1a/1b⁻/⁻* mice

	WT		*Slco1a/1b⁻/⁻*		
	Conc.	T/P ratio	Conc.	T/P ratio	WT/KO conc. ratio
Plasma (µg/ml)	0.22 ± 0.1	–	0.73 ± 0.1[A]	–	0.30
Liver (µg/g)	6.85 ± 1.2	31.8 ± 5.7	2.25 ± 0.3[A]	3.1 ± 0.3[A]	3.04
Kidney (µg/g)	3.93 ± 1.2	18.6 ± 7.3	5.50 ± 1.2	7.7 ± 2.0[B]	0.71
SI (+ contents) (µg/g)	4.51 ± 0.6	21.4 ± 6.2	2.80 ± 0.4[B]	3.9 ± 0.8[C]	1.61
Brain (µg/g)	0.05 ± 0.00	0.23 ± 0.06	0.07 ± 0.01[B]	0.10 ± 0.02[B]	0.71
Spleen (µg/g)	0.25 ± 0.06	1.31 ± 0.30	0.62 ± 0.14[C]	0.84 ± 0.09	0.40

[³H]FEX administered at 1 mg/kg. Data are presented as mean ± SD ($n = 4$–5). [A]$P < 0.001$; [B]$P < 0.01$; [C]$P < 0.05$ when compared with WT.

unexpected and, as discussed below, it could change our perspective on the functioning of the normal liver. We also found that Oatp1a/1b proteins are involved in the hepatic uptake of unconjugated bile acids. Furthermore, using this model we could demonstrate an important role of Oatp1a/1b proteins in the disposition of various drugs, mainly by their pronounced effect on the hepatic uptake of drugs.

Total bilirubin plasma levels in *Slco1a/1b⁻/⁻* mice were more than 40-fold increased compared with WTs. Remarkably, 95% of this increase could be ascribed to increased levels of conjugated bilirubin. Hepatic glucuronidation by Ugt1a1 is likely the most important detoxification pathway for bilirubin in mice, although it has to be noted that in humans gastrointestinal glucuronidation of bilirubin might also play a (minor) role (17). Bilirubin glucuronides formed within the liver can be transported into bile by Abcc2, Abcg2, and some other, as yet unidentified, canalicular transporter(s) (18, 19) or, under pathological conditions (cholestasis), back into the circulation by Abcc3 (15, 20). Our results lead us to hypothesize the unexpected existence of a substantial and, at first sight, seemingly futile cycling of bilirubin glucuronides in normal, healthy liver, in which bilirubin conjugated in the liver is substantially secreted across the sinusoidal membrane by Abcc3. We propose that the subsequent effective reuptake into the liver is mediated by Oatp1a/1b transporters. Interestingly, in the absence of Oatp1a/1b transporters, hepatobiliary elimination of bilirubin glucuronide was practically halved (Figure 2C), suggesting that under normal condi-

tions at least half of the bilirubin glucuronide formed in the liver undergoes sinusoidal secretion and reuptake.

These findings may alter our perspective on the detoxifying functioning of the normal liver. Rather than a mostly unidirectional process, bilirubin detoxification seems to be dynamic, with the flexibility to reroute glucuronidated bilirubin (and presumably many other conjugated compounds as well) formed in 1 hepatocyte to downstream hepatocytes by secretion via ABCC3 (21) and subsequent OATP1A/1B-mediated reuptake for final biliary excretion. We hypothesize that this "hepatocyte hopping" afforded by the tandem activity of ABCC3 and OATP1A/1B transporters can help to prevent saturation of the canalicular excretion of many conjugated compounds generated in the periportal hepatocytes, which are the first and most highly exposed to xenobiotics and endotoxins. Thus, sinusoidal back-transport of hepatic-conjugated compounds toward the blood by ABCC3 (and ABCC4) would not only be important during cholestasis to afford alternative renal excretion (22), but also during the normal functioning of the liver by allowing the distribution of the excretion load over the entire liver lobule.

An alternative explanation for the observed conjugated hyperbilirubinemia in *Slco1a/1b⁻/⁻* mice might be altered enterohepatic circulation of bilirubin-glucuronide, which, after reaching the portal blood, would be dependent on Oatp1a/1b transporters for the reuptake into the hepatocytes. However, although enterohepatic circulation of UCB has been demonstrated under some specific conditions (e.g., increased intestinal bile acid levels for
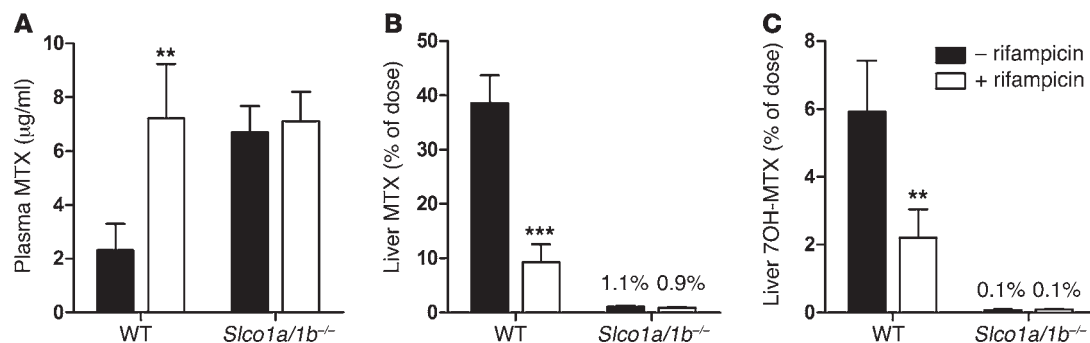
Figure 6

The effect of Oatp inhibition by rifampicin on MTX disposition in female WT and *Slco1a/1b⁻/⁻* mice. MTX plasma concentration (**A**), MTX liver levels (% of dose) (**B**), and 7OH-MTX liver levels (% of dose) (**C**) 15 minutes after i.v. administration of MTX (10 mg/kg) with or without predosing of rifampicin (20 mg/kg). If applicable, rifampicin or vehicle was administered i.v. 3 minutes before MTX administration. All data are presented as mean ± SD ($n = 5$; **$P < 0.01$; ***$P < 0.001$ when compared with vehicle treatment).

example during bile acid malabsorption) in rodents (23–25) and humans (26), enterohepatic circulation of conjugated bilirubin has never been demonstrated. We therefore consider this alternative hypothesis less plausible.

Another hypothesis would be that conjugated hyperbilirubinemia in *Slco1a/1b*−/− mice is somehow caused by the 2-fold decreased canalicular excretion of bilirubin-glucuronide into bile that we observed. Indeed, Abcc2-deficient mice also display a 2-fold reduced output of bilirubin-glucuronide, associated with mildly increased plasma levels of bilirubin-glucuronide (to about 4 μM) (18). Abcc2 is the main canalicular bilirubin-glucuronide exporter in mice, with an ancillary role of Abcg2 (19). However, we found that levels of Abcc2 and Abcg2 proteins are normal in the *Slco1a/1b*−/− mice, and it is not obvious why the activity of these transporters would be reduced: hepatic accumulation of potentially inhibiting compounds is more likely to be decreased than increased in the *Slco1a/1b*−/− mice, and there are also no indications for profound changes in hepatic expression of transporters (Supplemental Table 1). Also, biliary excretion of GSH, which is primarily mediated by Abcc2 (18, 19), is unchanged. This strongly supports normal activity of Abcc2 in the *Slco1a/1b*−/− mice. Finally, the plasma bilirubin-glucuronide level is much higher in the *Slco1a/1b*−/− mice (>45 μM) than in the *Abcc2*−/− mice (4 μM), despite similar levels of biliary bilirubin-glucuronide output. Reduced biliary excretion of bilirubin-glucuronide as a primary cause of the conjugated hyperbilirubinemia in *Slco1a/1b*−/− mice thus seems both mechanistically unlikely and insufficient to explain the data.

Our bilirubin data are in line with in vitro studies demonstrating that Oatp1a1 (27), OATP1B1, and OATP1B3 (28, 29) can transport bilirubin glucuronides with high affinity (K_m values < 0.5 μM). Furthermore, in humans the *SLCO1B1*1b* (Val174Ala), -*5* (Asp130Asn), and -*15* (Asp130Asn + Val174Ala) haplotypes have also been associated with significantly (albeit modestly) increased plasma levels of both conjugated bilirubin and UCB (30–33). Interestingly, results from the study by Sanna et al. suggested that SNPs in *SLCO1B1* were mostly associated with conjugated bilirubin, whereas an intronic polymorphism in *SLCO1B3* was mainly associated with mild unconjugated hyperbilirubinemia (31). In general, the fact that genetic variation in *SLCO1A/1B* genes is associated with increased levels of UCB (in addition to conjugated bilirubin) might point to possible species differences in hepatic uptake of UCB; we note that our data do not indicate an essential role of murine Oatp1a/1b transporters in the liver uptake of UCB, as most bilirubin was still effectively conjugated in *Slco1a/1b*−/− mice and therefore must have entered the hepatocytes. Also, UCB plasma levels were only slightly increased in *Slco1a/1b*−/− mice, which might be a consequence of some in vivo deconjugation of the circulating bilirubin-glucuronide. However, we cannot exclude that Oatp1a/1b proteins can make a nonessential contribution to UCB uptake into the liver. Whether one or more other sinusoidal uptake transporters, or passive diffusion, are primarily responsible for the UCB uptake into hepatocytes remains an open question.

Bile acids play an important role in several physiological processes and they are therefore subject to strict homeostasis (34). Bile acids are synthesized from cholesterol in the liver and undergo extensive enterohepatic circulation, a process in which Na+ taurocholate cotransporting polypeptide (NTCP), bile acid export pump (BSEP/ABCB11), apical sodium bile acid transporter (ASBT), and organic solute transporter (OST$_\alpha$/OST$_\beta$) play important roles (reviewed in refs. 35, 36). Although it is widely accepted that NTCP/

Ntcp functions as the main hepatic bile acid uptake transporter, *Slco1a/1b*−/− mice showed markedly increased levels of total bile acids in plasma, and this was almost exclusively due to increased unconjugated bile acid levels (13-fold increased; Figure 2B and Supplemental Figure 1). These results suggest that in vivo, conjugated bile acids are primarily taken up by Ntcp and unconjugated bile acids by Oatp1a/1b (note that expression of Ntcp was not changed in *Slco1a/1b*−/− mice; Supplemental Table 1). Indeed, in vitro studies with rat hepatocytes showed that Na+-dependent transport dominated the uptake of the conjugated bile acid taurocholate (>80%), whereas unconjugated bile acids were more efficiently taken up by (one or more) Na+-independent transport systems, which could include Oatps (36, 37). We note that unconjugated bile acids only account for a small fraction of the overall bile acid pool in the body, which might explain the unchanged biliary excretion of total bile acids in *Slco1a/1b*−/− mice that we observed. Together, our data demonstrate that Oatp1a/1b transporters make a substantial contribution to hepatic (re-)uptake of unconjugated but not conjugated bile acids. Partly in line with these results, Xiang et al. recently showed that individuals with the *SLCO1B1*5* haplotype have increased plasma levels of unconjugated and conjugated bile acids (33).

The present study demonstrates that Oatp1a/1b transporters play an essential role in the pharmacokinetics of MTX and FEX by mediating most of the hepatic uptake of these compounds. Interestingly, the effect of Oatp1a/1b transporters was virtually instantaneous, and only 3.5 minutes after i.v. injection of MTX and FEX, we observed profoundly increased plasma levels in *Slco1a/1b*−/− mice and profoundly decreased liver levels of MTX and FEX. Moreover, WT mice showed high liver-to-plasma ratios of MTX and FEX 15 minutes after administration (ratios of 43 and 32, respectively; Tables 1 and 2), whereas in *Slco1a/1b*−/− mice, these values were below 4. This suggests not only that Oatp1a/1b transporters have a high capacity to transport these drugs, but also that they may actively concentrate these drugs in the liver. In vitro studies have shown that MTX is a substrate for Oatp1a4, OATP1B1, OATP1B3, and OATP1A2 (12–14). FEX is transported in vitro by Oatp1a1, -1a4, -1a5 and -1b2, and OATP1A2 (38, 39), but in vitro studies of OATP1B1 and -1B3-mediated uptake of FEX are quite inconsistent (39–41). In the present study, by using *Slco1a/1b*−/− mice, we proved that Oatp1a/1b transporters effect a profound impact on MTX and FEX pharmacokinetics by acting as high-capacity hepatic uptake transporters that determine the overall elimination rate of these drugs. Note that the plasma levels of the drugs obtained in these mouse studies were well within the therapeutic range in humans.

Surprisingly, shortly after oral dosing of MTX and FEX, no first-pass effect of hepatic Oatp1a/1b transporters was observed, since at those time points plasma and liver concentrations of the drugs did not differ between WT and *Slco1a/1b*−/− mice. This is in contrast to the rapid and profound effect of hepatic Oatp1a/1b transporters after i.v. administration of MTX and FEX. A possible explanation might be that because of the effectively approximately 100-fold lower plasma concentrations of the drugs upon intestinal uptake compared with shortly after bolus i.v. injection (Figures 3 and 5), there is much more extensive plasma protein binding of the drugs, reducing the drug fraction immediately available for hepatic uptake. Another possibility might be that shortly after oral dosing, concentrations of the drugs in the portal vein are low compared with the K_m values of Oatp1a/1b, allowing other hepatic uptake

transporters with higher affinities but lower capacities to mediate most hepatic drug uptake. Indeed, for the transport of FEX by hepatic Oatp1a1 and Oatp1a4, the K_m values are 32 and 6 µM (38), respectively, and portal vein concentrations of FEX are far below these K_m values (~0.03–0.09 µM; Figure 5).

Slco1a/1b−/− mice did not display reduced intestinal absorption of MTX and FEX upon oral dosing, despite the fact that we could demonstrate *Slco1a4* and some *Slco1a6* mRNA in the small intestine. In vitro, Oatp1a4 can transport both MTX and FEX (14, 39). An explanation for this might be the intestinal expression of Oatp2b1, which possibly compensates for the lack of Oatp1a/1b transporters or the presence of other intestinal uptake transporters. In addition, MTX is transported by the reduced folate carrier (RFC1) which is also present at the apical membrane of mouse small intestinal enterocytes (but not in hepatocytes) (42, 43). Intestinal absorption of MTX in mice might therefore be primarily mediated by RFC1 rather than Oatp1a/1b transporters. Nevertheless, Oatp1a/1b function does have a profound impact on overall oral availability of MTX and FEX (Figures 3 and 5), most likely by its effect on the hepatic elimination of these drugs.

We could demonstrate extensive in vivo inhibition of Oatp1a/1b by rifampicin. Previous in vitro studies have shown that rifampicin is an inhibitor of Oatp1a4, Oatp1b2, OATP1B1, and OATP1B3 (44–46). Rifampicin, an antibiotic mainly used in the treatment of tuberculosis, has been shown to reduce the elimination of BSP and to increase serum-conjugated bilirubin and UCB levels (30, 47). Importantly, our results indicate that rifampicin is quite Oatp1a/1b specific in vivo (at least in the context of MTX pharmacokinetics), since rifampicin treatment did not affect liver or plasma levels of MTX in *Slco1a/1b−/−* mice. These data demonstrate that *Slco1a/1b−/−* mice present an ideal tool to study the efficacy and specificity of (novel) Oatp1a/1b inhibitors.

The results of this study and the mouse model generated for it might have important implications for drug development and drug therapy. Although *Slco1b2−/−* mice have already shown the impact of hepatic Oatp1b2 on liver uptake of some toxins, statins, and antibiotics (2, 9, 10), in this study we demonstrated that Oatp1a/1b effects an even more profound impact on drug pharmacokinetics by mediating (for some drugs, virtually all) hepatic uptake of drugs. This might have sweeping consequences for drug pharmacokinetics in patients, since many SNPs have been identified in the *SLCO1B1*, *SLCO1B3*, and *SLCO1A2* genes, some of which are responsible for markedly reduced transport capacities (reviewed in ref. 6). For example, individuals carrying *SLCO1B1*15* (388A>G and 521T>C) have markedly increased plasma levels of statins and are at increased risk of developing statin-induced myopathy (6, 7). *SLCO1B1*15* has also been associated with life-threatening toxicities in patients treated with irinotecan (8). Moreover, 2 intronic SNPs in *SLCO1B1*, which are linked to each other and to 521T>C, were recently associated with increased plasma clearance and gastrointestinal toxicity of MTX (mucositis grade 3 or 4) (48). This could imply that individualized therapy, based on *SLCO* genotype, might partly overcome interindividual variation. This latter phenomenon is causing problems in the clinic, since many drugs (and especially anticancer drugs) have a narrow therapeutic window.

Our results indicate that coadministration of a specific OATP inhibitor could be used to increase systemic exposure and hence oral availability of drugs that otherwise have high OATP1A/1B-mediated hepatic uptake. Furthermore, inhibition of OATP1A/1B

transporters might be used to limit hepatic toxicity of some drugs. However, adverse drug reactions elsewhere in the body might occur when drugs reach toxic plasma levels upon (unintentional) coadministration with an OATP inhibitor. The *Slco1a/1b−/−* mice will be invaluable tools in studying the consequences of *SLCO1B* deficiencies and in testing OATP1A/1B modulation strategies.

In conclusion, we have shown that the Oatp1a/1b knockout mouse model presents a powerful tool in studying the role of Oatp1a/1b transporters in liver physiology and drug pharmacokinetics. We expect that this mouse model will be of great value during drug development and optimization of drug therapy, especially when complemented with transgenic expression of individual human OATP1A/1B transporters to create humanized mouse models.

Methods

Animals. Mice were housed and handled according to institutional guidelines. All mouse experiments were approved by the Animal Experiments Review Board of the Netherlands Cancer Institute (Amsterdam), complying with Dutch legislation. The animals used in this study were *Slco1a/1b−/−* and WT mice of comparable mixed genetic background (approximately 50% 129/Ola, 50% FVB) between 9 and 14 weeks of age. Animals were kept in a temperature-controlled environment with a 12-hour light/12-hour dark cycle. They received a standard diet (AM-II; Hope Farms) and acidified water ad libitum.

Generation of Slco1a/1b−/− mice. Construction of targeting vectors, generation, and PCR and Southern blot analysis of *Slco1a/1b−/−* mice are described in Supplemental Methods and (partly) presented in Figure 1A.

Analysis of bilirubin, bile acids, and GSH in plasma, bile, and urine. Gallbladder cannulations and collection of bile in male WT and *Slco1a/1b−/−* mice (*n* = 6–7) were performed as described (18). We also collected urine (spot collection beforehand) and heparin plasma (cardiac puncture afterwards) from these mice. For the detection of plasma bile acids, another set of male WT and *Slco1a/1b−/−* mice (*n* = 5–6) was used. Ascorbate (100 mg/ml) was added to all plasma (10 µl), urine (10 µl), and bile samples (2 µl) in order to prevent oxidation of bilirubin. Concentrations of BMG, BDG, and UCB in bile were determined by reverse-phase HPLC as described (49). Bile was injected after dilution (20 times) with water. For the detection of BMG, BDG, and UCB in plasma and urine, the protocol described in Supplemental Methods was adapted. Bile acids in plasma and bile, and GSH in bile were determined as described (50). Determination of the total bile acid pool is described in Supplemental Methods.

Plasma and tissue pharmacokinetic experiments. For i.v. administration of MTX, 5 µl of drug solution (2 mg/ml in saline) per gram of body weight was injected into the tail vein of female mice (*n* = 4–7 for each group). When indicated, 5 µl of rifampicin (4 mg/ml in saline) per gram of body weight was injected into the tail vein 3 minutes before MTX administration. For oral administration, MTX was formulated in 5% (w/v) D-glucose at 1 mg/ml and 10 µl drug solution/g body weight was dosed by oral gavage into the stomach of female mice (*n* = 4–8 for each group). [3H]FEX was i.v. administered by injecting 5 µl of the drug solution (0.2 mg/ml in saline) per gram of body weight into the tail vein of male mice (*n* = 4–5 for each group). For oral administration, [3H]FEX was formulated in 5% (w/v) D-glucose at 0.1 mg/ml and 10 µl drug solution/g body weight was dosed by oral gavage into the stomach of male mice (*n* = 4–5 for each group).

For all i.v. experiments, animals were sacrificed at indicated time points by terminal bleeding through cardiac puncture under methoxyflurane anesthesia and tissues were isolated. After oral administration, mice were anesthetized by methoxyflurane and, at indicated time points, heparin blood samples were taken from the portal vein directly followed

by cardiac puncture and isolation of tissues. Blood samples were centrifuged at 2,700 g for 5 minutes at 4°C, and plasma was collected and stored at –20°C until analysis.

Urinary and fecal excretion of MTX. A mass balance study was performed with Ruco Type M/1 stainless steel metabolic cages (Valkenswaard). Male WT and *Slco1a/1b⁻/⁻* mice (n = 6 for each group) were allowed to become accustomed to the cages for 24 hours before receiving MTX (10 mg/kg) injected into the tail vein. Urine and feces were collected in a 0–24 hour fraction after drug administration. At the end of the experiment, mice were killed by terminal bleeding through cardiac puncture under methoxyflurane anesthesia.

Drug analysis. Amounts of MTX and 7OH-MTX in plasma, urine, feces, and organs (homogenized in ice-cold 4% [w/v] BSA using a Polytron homogenizer) were determined by HPLC analysis as described (51). Levels of [³H]FEX in plasma and organs were determined by scintillation counting (Tri-Carb 2100 CS Liquid Scintillation Analyzer, Canberra Packard). The organs were first incubated overnight at 65°C in Solvable (PerkinElmer). To decolorize the solution, appropriate amounts of 30% H_2O_2 were added to the samples, followed by 10 ml Ultima Gold (Packard Bioscience BV).

Pharmacokinetic calculations and statistical analysis. The 2-sided unpaired Student's t test was used throughout the study to assess the statistical significance of differences between 2 sets of data. Results are presented as the mean ± SD. Differences were considered to be statistically significant when $P < 0.05$. Averaged concentrations for each time point were used to calculate the area under the plasma concentration versus time curve (AUC) from t = 0 to the last sampling time point by the linear trapezoidal rule; SEM was calculated by the law of propagation of errors (52). Results of the AUC measurements are presented as mean ± SEM.

1. Hagenbuch B, Meier PJ. Organic anion transporting polypeptides of the OATP/ SLC21 family: phylogenetic classification as OATP/ SLCO superfamily, new nomenclature and molecular/functional properties. *Pflügers Arch.* 2004;447(5):653–665.
2. Evers R, Chu XY. Role of the murine organic anion-transporting polypeptide 1b2 (Oatp1b2) in drug disposition and hepatotoxicity. *Mol Pharmacol.* 2008;74(2):309–311.
3. Niemi M. Role of OATP transporters in the disposition of drugs. *Pharmacogenomics.* 2007;8(7):787–802.
4. Kalliokoski A, Niemi M. Impact of OATP transporters on pharmacokinetics. *Br J Pharmacol.* 2009;158(3):693–705.
5. Hagenbuch B, Gui C. Xenobiotic transporters of the human organic anion transporting polypeptides (OATP) family. *Xenobiotica.* 2008;38(7-8):778–801.
6. König J, Seithel A, Gradhand U, Fromm MF. Pharmacogenomics of human OATP transporters. *Naunyn Schmiedebergs Arch Pharmacol.* 2006;372(6):432–443.
7. Morimoto K, Oishi T, Ueda S, Ueda M, Hosokawa M, Chiba K. A novel variant allele of OATP-C (SLCO1B1) found in a Japanese patient with pravastatin-induced myopathy. *Drug Metab Pharmacokinet.* 2004;19(6):453–455.
8. Takane H, et al. Life-threatening toxicities in a patient with UGT1A1*6/*28 and SLCO1B1*15/*15 genotypes after irinotecan-based chemotherapy. *Cancer Chemother Pharmacol.* 2009; 63(6):1165–1169.
9. Lu H, et al. Characterization of organic anion transporting polypeptide 1b2-null mice: essential role in hepatic uptake/toxicity of phalloidin and microcystin-LR. *Toxicol Sci.* 2008;103(1):35–45.
10. Zaher H, et al. Targeted disruption of murine organic anion-transporting polypeptide 1b2 (Oatp1b2/Slco1b2) significantly alters disposition of prototypical drug substrates pravastatin and rifampin. *Mol Pharmacol.* 2008;74(2):320–329.
11. van de Steeg E, et al. Methotrexate pharmacokinetics in transgenic mice with liver-specific expression of human OATP1B1 (SLCO1B1). *Drug Metab Dispos.* 2008;37(1):1–5.
12. Abe T, et al. LST-2, a human liver-specific organic anion transporter, determines methotrexate sensitivity in gastrointestinal cancers. *Gastroenterology.* 2001;120(7):1689–1699.
13. Badagnani I, et al. Interaction of methotrexate with organic-anion transporting polypeptide 1A2 and its genetic variants. *J Pharmacol Exp Ther.* 2006;318(2):521–529.
14. Sasaki M, Suzuki H, Aoki J, Ito K, Meier PJ, Sugiyama Y. Prediction of in vivo biliary clearance from the in vitro transcellular transport of organic anions across a double-transfected Madin-Darby canine kidney II monolayer expressing both rat organic anion transporting polypeptide 4 and multidrug resistance associated protein 2. *Mol Pharmacol.* 2004;66(3):450–459.
15. Vlaming ML, et al. Impact of Abcc2 (Mrp2) and Abcc3 (Mrp3) on the in vivo elimination of methotrexate and its main toxic metabolite 7-hydroxymethotrexate. *Clin Cancer Res.* 2008;14(24):8152–8160.
16. Tahara H, Kusuhara H, Fuse E, Sugiyama Y. P-glycoprotein plays a major role in the efflux of fexofenadine in the small intestine and blood-brain barrier, but only a limited role in its biliary excretion. *Drug Metab Dispos.* 2005;33(7):963–968.
17. Chen S, et al. Tissue-specific, inducible, and hormonal control of the human UDP-glucuronosyltransferase-1 (UGT1) locus. *J Biol Chem.* 2005;280(45):37547–37557.
18. Vlaming ML, et al. Carcinogen and anticancer drug transport by Mrp2 in vivo: studies using Mrp2 (Abcc2) knockout mice. *J Pharmacol Exp Ther.* 2006;318(1):319–327.
19. Vlaming ML, et al. Functionally overlapping roles of Abcg2 (Bcrp1) and Abcc2 (Mrp2) in the elimination of methotrexate and its main toxic metabolite 7-hydroxymethotrexate in vivo. *Clin Cancer Res.* 2009;15(9):3084–3093.
20. Zelcer N, et al. Mice lacking Mrp3 (Abcc3) have normal bile salt transport, but altered hepatic transport of endogenous glucuronides. *J Hepatol.* 2006;44(4):768–775.
21. Lee YM, et al. Identification and functional characterization of the natural variant MRP3-Arg1297His of human multidrug resistance protein 3 (MRP3/ ABCC3). *Pharmacogenetics.* 2004;14(4):213–223.
22. Zollner G, Trauner M. Molecular mechanisms of cholestasis. *Wien Med Wochenschr.* 2006; 156(13-14):380–385.
23. Brink MA, Mendez-Sanchez N, Carey MC. Bilirubin cycles enterohepatically after ileal resection in the rat. *Gastroenterology.* 1996;110(6):1945–1957.
24. Mendez-Sanchez N, Brink MA, Paigen B, Carey MC. Ursodeoxycholic acid and cholesterol induce enterohepatic cycling of bilirubin in rodents. *Gastroenterology.* 1998;115(3):722–732.
25. Lester R, Schmid R. Intestinal absorption of bile pigments. II. Bilirubin absorption in man. *N Engl J Med.* 1963;269:178–182.
26. Lester R, Schmid R. Intestinal absorption of bile pigments. I. The enterohepatic circulation of bilirubin in the rat. *J Clin Invest.* 1963;42:736–746.
27. Reichel C, et al. Localization and function of the organic anion-transporting polypeptide Oatp2 in rat liver. *Gastroenterology.* 1999;117(3):688–695.
28. Cui Y, König J, Leier I, Buchholz U, Keppler D. Hepatic uptake of bilirubin and its conjugates by the human organic anion transporter SLC21A6. *J Biol Chem.* 2001;276(13):9626–9630.
29. König J, Cui Y, Nies AT, Keppler D. A novel human organic anion transporting polypeptide localized to the basolateral hepatocyte membrane. *Am J Physiol Gastrointest Liver Physiol.* 2000;278(1):G156–G164.
30. Zhang W, et al. OATP1B1 polymorphism is a major determinant of serum bilirubin level but not associated with rifampicin-mediated bilirubin elevation. *Clin Exp Pharmacol Physiol.* 2007;34(12):1240–1244.
31. Sanna S, et al. Common variants in the SLCO1B3 locus are associated with bilirubin levels and unconjugated hyperbilirubinemia. *Hum Mol Genet.* 2009;18(14):2711–2718.
32. Pasanen MK, Neuvonen PJ, Niemi M. Global analysis of genetic variation in SLCO1B1. *Pharmacogenomics.* 2008;9(1):19–33.
33. Xiang X, et al. Effect of SLCO1B1 polymorphism on the plasma concentrations of bile acids and bile acid synthesis marker in humans. *Pharmacogenet Genomics.* 2009;19(6):447–457.
34. Monte MJ, Marin JJ, Antelo A, Vazquez-Tato J. Bile acids: chemistry, physiology, and pathophysiology. *World J Gastroenterol.* 2009;15(7):804–816.
35. Meier PJ, Stieger B. Bile salt transporters. *Annu Rev Physiol.* 2002;64:635–661.
36. Dawson PA, Lan T, Rao A. Bile acid transporters. *J Lipid Res.* 2009;50(12):2340–2357.
37. Meier PJ, Eckhardt U, Schroeder A, Hagenbuch B, Stieger B. Substrate specificity of sinusoidal bile acid and organic anion uptake systems in rat and human liver. *Hepatology.* 1997;26(6):1667–1677.
38. Cvetkovic M, Leake B, Fromm MF, Wilkinson GR, Kim RB. OATP and P-glycoprotein transporters mediate the cellular uptake and excretion of fexofenadine. *Drug Metab Dispos.* 1999;27(8):866–871.
39. Glaeser H, et al. Intestinal drug transporter expression and the impact of grapefruit juice in humans. *Clin Pharmacol Ther.* 2007;81(3):362–370.

40. Shimizu M, et al. Contribution of OATP (organic anion-transporting polypeptide) family transporters to the hepatic uptake of fexofenadine in humans. *Drug Metab Dispos*. 2005;33(10):1477–1481.

41. Matsushima S, Maeda K, Ishiguro N, Igarashi T, Sugiyama Y. Investigation of the inhibitory effects of various drugs on the hepatic uptake of fexofenadine in humans. *Drug Metab Dispos*. 2008;36(4):663–669.

42. Kneuer C, Honscha KU, Honscha W. Rat reduced-folate carrier-1 is localized basolaterally in MDCK kidney epithelial cells and contributes to the secretory transport of methotrexate and fluoresceinated methotrexate. *Cell Tissue Res*. 2005;320(3):517–524.

43. Wang Y, Zhao R, Russell RG, Goldman ID. Localization of the murine reduced folate carrier as assessed by immunohistochemical analysis. *Biochim Biophys Acta*. 2001;1513(1):49–54.

44. Fattinger K, Cattori V, Hagenbuch B, Meier PJ, Stieger B. Rifamycin SV and rifampicin exhibit differential inhibition of the hepatic rat organic anion transporting polypeptides, Oatp1 and Oatp2. *Hepatology*. 2000;32(1):82–86.

45. Lau YY, Okochi H, Huang Y, Benet LZ. Multiple transporters affect the disposition of atorvastatin and its two active hydroxy metabolites: application of in vitro and ex situ systems. *J Pharmacol Exp Ther*. 2006;316(2):762–771.

46. Vavricka SR, Van Montfoort J, Ha HR, Meier PJ, Fattinger K. Interactions of rifamycin SV and rifampicin with organic anion uptake systems of human liver. *Hepatology*. 2002;36(1):164–172.

47. Corpechot C, Ping C, Wendum D, Matsuda F, Barbu V, Poupon R. Identification of a novel 974C->G nonsense mutation of the MRP2/ABCC2 gene in a patient with Dubin-Johnson syndrome and analysis of the effects of rifampicin and ursodeoxycholic acid on serum bilirubin and bile acids. *Am J Gastroenterol*. 2006;101(10):2427–2432.

48. Trevino LR, et al. Germline genetic variation in an organic anion transporter polypeptide associated with methotrexate pharmacokinetics and clinical effects. *J Clin Oncol*. 2009;27(35):5972–5978.

49. Spivak W, Carey MC. Reverse-phase h.p.l.c. separation, quantification and preparation of bilirubin and its conjugates from native bile. Quantitative analysis of the intact tetrapyrroles based on h.p.l.c. of their ethyl anthranilate azo derivatives. *Biochem J*. 1985;225(3):787–805.

50. Bootsma AH, et al. Rapid analysis of conjugated bile acids in plasma using electrospray tandem mass spectrometry: application for selective screening of peroxisomal disorders. *J Inherit Metab Dis*. 1999;22(3):307–310.

51. van Tellingen O, van der Woude HR, Beijnen JH, van Beers CJ, Nooyen WJ. Stable and sensitive method for the simultaneous determination of N5-methyltetrahydrofolate, leucovorin, methotrexate and 7-hydroxymethotrexate in biological fluids. *J Chromatogr*. 1989;488(2):379–388.

52. Bardelmeijer HA, et al. Increased oral bioavailability of paclitaxel by GF120918 in mice through selective modulation of P-glycoprotein. *Clin Cancer Res*. 2000;6(11):4416–4421.